

Simple Ligand Modifications with Pendent OH Groups Dramatically Impact the Activity and Selectivity of Ruthenium Catalysts for Transfer Hydrogenation: The Importance of Alkali Metals

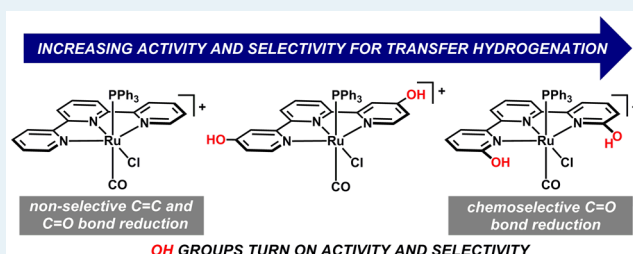
Cameron M. Moore, Byongjoo Bark, and Nathaniel K. Szymczak*

Department of Chemistry, University of Michigan, 930 North University, Ann Arbor, Michigan 48109, United States

Supporting Information

ABSTRACT: Remarkable differences in selectivity and activity for ruthenium-catalyzed transfer hydrogenation are described that are imparted by pendent OH groups. Kinetic experiments, as well as the study of control complexes devoid of OH groups, reveal that the pendent OH groups serve to orient the ketone substrate through ion pairing with an alkali metal under basic conditions. The deprotonation of the OH groups was found to modulate the electronics at the metal center, providing a more electron rich ruthenium center. The effects of the ion pairing between alkali metals and the pendent alkoxide groups were highlighted by demonstrating chemoselective transfer hydrogenation of ketones in the presence of olefins. The results illustrate that a simple ligand modification (installation of OH groups) imparts dramatic changes to catalysis. Pendent OH groups turn on catalysis through electronic perturbations at the metal site under basic conditions and can also change the mechanism of catalysis, the latter of which can be used to promote chemoselective reductions.

KEYWORDS: secondary coordination sphere, alkali metals, ion pairing, ruthenium, transfer hydrogenation



INTRODUCTION

Metal–ligand bifunctionality has become a powerful design concept upon which efficient catalysts used in a wide variety of chemical transformations have been constructed.¹ Key to the function is the ability of the ligand framework to adopt two (or more) distinct states which can modulate the electronic configuration of the metal center, accept/donate protons, engage in ion pairing, and induce conformational changes to the primary coordination sphere (Figure 1).¹ These concepts are perhaps best illustrated with Noyori's hydrogenation catalysts, which feature ruthenium amine units to facilitate cooperative H₂ activation and transfer.² Following blueprints outlined by Noyori and related outer-sphere catalysts, systems

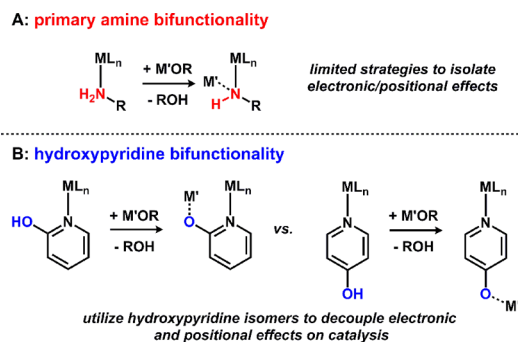


Figure 1. Comparison of metal–ligand bifunctionality with primary amine (A) and hydroxypyridine ligand motifs (B).

that operate through metal/ligand bifunctional pathways have recently seen a surge in activity.³ However, the successful incorporation of appended functionality to impart efficient catalysis has been less straightforward, and multifunctional complexes that also feature high catalytic activity have been challenging to predict a priori. In many cases, an active catalyst undergoes a series of steric and electronic changes imparted by the reaction media, which in turn afford an active catalyst structure that may or may not bear a high resemblance to the starting state.⁴ Proximity, high directionality, and electronic effects are all required to work synergistically in order to effect efficient catalysis.⁵

Although the benefits of ligand NH₂ groups on catalytic activity were realized in the case of Noyori's catalyst, the intimate details of the “NH effect”⁶ in this complex have not been well understood until recently. During hydrogenation catalysis, the deprotonated NH group of the diamine ligand in Noyori's catalyst was originally proposed to be directly responsible for H₂ heterolysis: proceeding through a four-membered transition state in which a hydride (H[−]) is transferred to the metal center and H⁺ is transferred to the amine ligand (Figure 2A).⁷

More recently, however, this supposition has been debated in the literature and contemporary experimental evidence suggests that a four-membered transition state for H₂ heterolysis is

Received: January 23, 2016

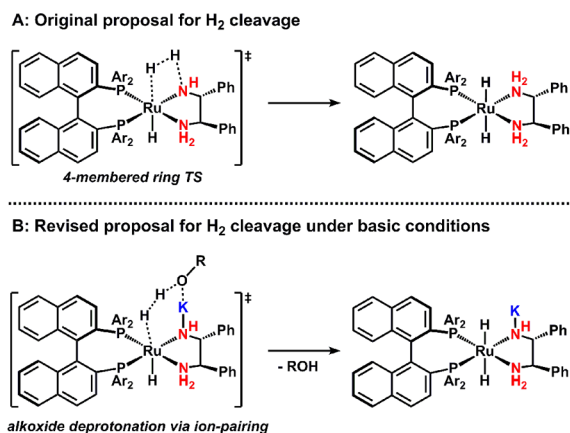


Figure 2. Original (A) and revised (B) proposals for H₂ cleavage by Noyori's catalyst during catalysis.

unlikely to be operative under basic conditions. In fact, later studies revealed that an alkali-metal “cocatalyst” is required to achieve high activity for ketone hydrogenation, and the activity of Noyori's catalyst is dependent on the identity of alkali metals added to the reaction mixture.⁸ Subsequent studies implicated a mechanism in which the alkali metal is bound to the deprotonated amine ligand during catalysis, generating an ion pair (Figure 2B).⁹ Importantly, recent computational analyses demonstrated that a four-membered transition state for H₂ heterolysis is not the lowest energy pathway under simulated catalytic conditions.¹⁰ Instead, H₂ cleavage was proposed to occur through an ion-pair alkoxide formed after hydride transfer to the ketone substrate. These studies demonstrate the complexity associated with predicting an active catalyst state, even from a deceptively simple ligand arrangement in the precatalyst.¹⁰

We, among others, have been working to design metal–ligand constructs with pendent functionality that can be widely deployed to facilitate an array of chemical transformations, including catalysis involving proton transfer.^{5a,c,11} To clearly delineate many of the key contributors to a productive cooperative catalyst, our group has undertaken efforts to understand how the precise structural, electronic, and cooperative modes of a metal's secondary coordination sphere can be used to regulate reactivity.^{11o} Our approach is to adapt key structural design criteria from metalloenzymes,¹² where the concept of metal–ligand bifunctionality has long been established to be vital for function.¹³ The 2-hydroxypyridine motif provides an ideal ligand platform for studying metal–ligand bifunctional reactivity, since the 4-hydroxypyridine isomer can be used as a control to decouple electronic and positional effects (Figure 1B). This strategy has previously been used to understand how pendent OH groups on bipyridine fragments effect oxidative and reductive catalysis.^{5a,b,d,11j,k,14} For catalysis applications, we developed a rigid terpyridine pincer framework incorporating the 2-hydroxypyridine motif (6,6'-dihydroxyterpyridine, dhtp),^{11a} which we envisioned could exploit appended O(H) groups to facilitate cooperative substrate reduction.

In this article, we build on our initial report and present transfer hydrogenation catalysis that is substantially amplified using well-positioned pendent OH groups on a terpyridine scaffold. The OH groups serve to turn on catalytic activity and chemoselective reduction reactions by modifying the electronic environment of the metal center upon deprotonation and

providing a precise spatial orientation of the substrate, directed by ion-pair interactions with alkali metals. Moreover, we demonstrate that both the presence and location of the pendent OH groups serve to dictate the activity and selectivity of ketone reduction and provide experimental evidence for a general alkoxide effect during catalysis in the presence of alkali metals.

RESULTS AND DISCUSSION

Pendent OH Groups Amplify Catalysis. We previously reported the synthesis and catalytic activity of a ruthenium complex supported by dhtp and two mutually trans PPh₃ ligands (*trans*-RuCl(dhtp)(PPh₃)₂PF₆, **1**).^{11a} This complex catalyzes transfer hydrogenation of a variety of ketones in the presence of several functional groups. Moreover, we demonstrated that the active species during catalysis is homogeneous and retains both PPh₃ ligands.^{11a} In order to interrogate the precise role of appended OH groups on catalysis, we investigated the “parent” terpyridine complex (*trans*-RuCl(terpy)(PPh₃)₂PF₆)¹⁵ for acetophenone transfer hydrogenation.

Under identical conditions (0.5 mol % of catalyst, 10 mol % of KO^tBu, ^tPrOH, 80 °C), the parent terpyridine complex exhibits diminished catalysis in comparison to the dhtp complex **1** (Figure 3A). While complex **1** provided

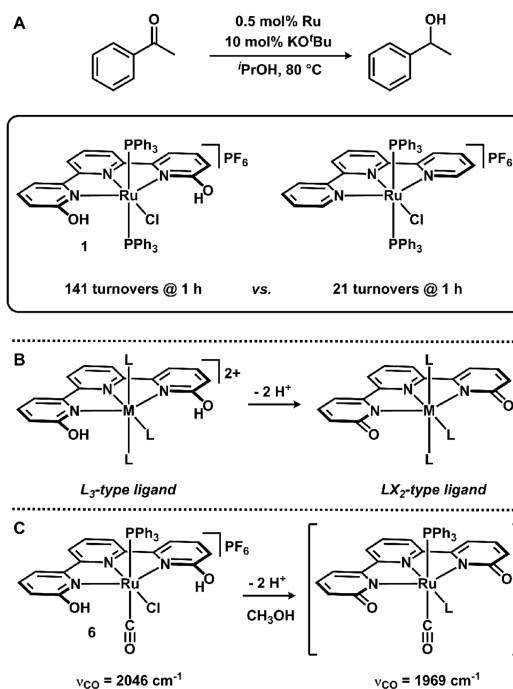


Figure 3. Comparison of dhtp and terpy for transfer hydrogenation (A), change of ligand classification upon deprotonation of dhtp (B), and observed changes in carbonyl stretching frequency upon addition of base to **6** in methanol solvent (C; L is most likely coordinated CH₃OH).

approximately 70% conversion of acetophenone to 1-phenylethanol (corresponding to 141 turnovers) in 1 h, the parent terpyridine complex only provided ~10% conversion (21 turnovers) over the same time period (Figure 3A). This amplification of catalysis highlights the regulatory role of pendent OH groups, and we hypothesized that the enhanced catalysis may be due to electronic differences between the two ligands under the reaction conditions. In the starting complex,

dhtp presents a neutral, L₃-type ligand; however, upon deprotonation and tautomerization, the dhtp ligand presents the metal center with a dianionic LX₂-type donor (Figure 3B). To evaluate this electronic effect, we examined the IR spectral changes for a variant of complex 1, RuCl(CO)dhtp(PPh₃)PF₆ (complex 6, vide infra), in which a PPh₃ ligand is substituted for CO. The ν_{CO} band of complex 6 was found to be sensitive to the presence of added base. For instance, the IR spectrum of 6 reveals a carbonyl stretching frequency of 2046 cm⁻¹. Upon treatment with 4 equiv of a strong, neutral base (Verkade's base; 2,8,9-triisopropyl-2,5,8,9-tetraaza-1-phosphabicyclo[3.3.3]undecane) in methanol solution, a shift of the carbonyl stretching frequency to 1969 cm⁻¹ was observed (Figure 3C). The bathochromic shift is consistent with increased electron density at the metal center and greater donation into the CO π* orbitals upon ligand deprotonation. The bathochromic shift (Δν = -77 cm⁻¹) is greater in magnitude than that observed for a copper(I)-carbonyl complex featuring a single 2-hydroxypyridine group (Δν = -26 cm⁻¹)¹⁶ but similar to that for a deprotonation of two alcohol ligands on iron (Δν = -69 cm⁻¹)¹⁷ and is therefore consistent with two deprotonation events for the dhtp ligand.

PPh₃ Ligand Substitution Modulates Catalyst Stability and Activity. During the course of our subsequent studies on ketone transfer hydrogenation catalyzed by 1, it became apparent that the efficiency of 1 was impeded by catalyst deactivation. This was evident by the formation of a deeply colored precipitate emerging as the reaction neared completion. Fortunately, we were able to isolate this material and identify the structure of the deactivation product through solution (NMR) and solid-state (X-ray) techniques (Figure 4).

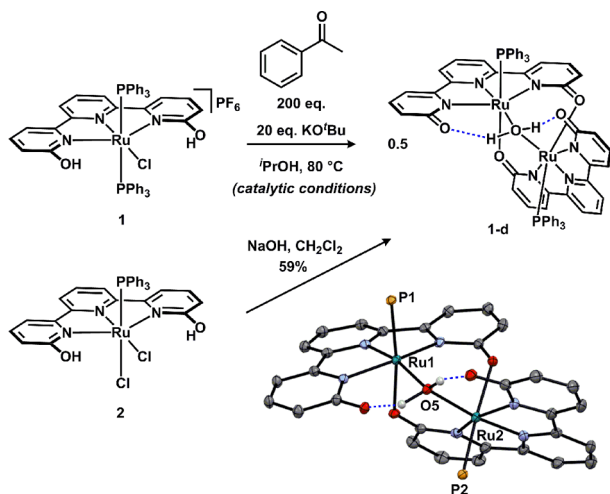


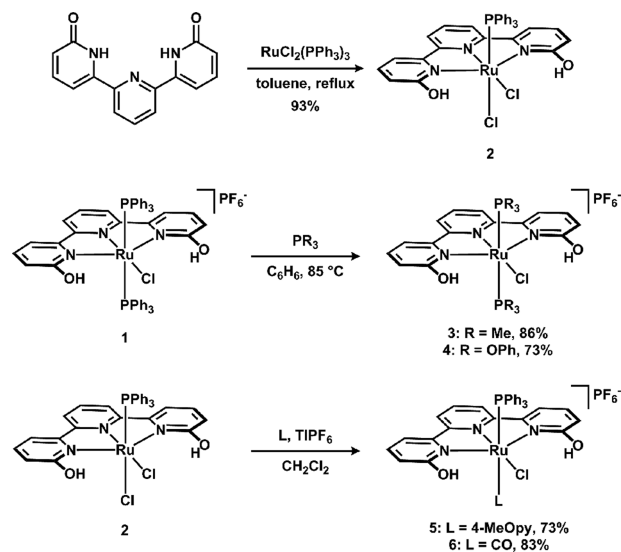
Figure 4. Synthesis and solid-state structure of 1-d (30% probability ellipsoids; PPh₃ C atoms, H atoms not involved in hydrogen bonding, and solvent omitted for clarity).

The deactivation product (1-d) is a ruthenium aquo-bridged dimer in which the Ru-(OH)₂-Ru unit is stabilized by intramolecular hydrogen-bonding interactions with the deprotonated dhtp ligand scaffold. Complex 1-d could alternatively be prepared by allowing *cis*-RuCl₂(dhtp)PPh₃ (2) to react with NaOH (Figure 4). Although the solvent used during catalysis (iPrOH) was distilled from CaH₂ and dried over activated molecular sieves prior to use, any adventitious water in solution presents a significant hurdle for achieving efficient catalysis,

since this deactivation product is highly stable and inert to ligand substitution.¹⁸

We hypothesized that catalyst activity could be optimized by modifying the auxiliary ligands on ruthenium and therefore prepared a series of complexes with varied donor sets. Two classes of complexes were synthesized (Scheme 1): one class

Scheme 1. Synthesis of Ruthenium-dhtp Adducts



featuring identical auxiliary ligands (3 and 4) and the other with dissimilar auxiliary ligands (5 and 6). Complexes 3 and 4 were prepared by heating benzene solutions of 1 with the appropriate PR₃ ligand in a sealed vessel. Complexes 5 and 6 were prepared by allowing complex 2 (prepared from the direct reaction of dhtp with RuCl₂(PPh₃)₃ in a nonpolar solvent at high temperature) to react with TIPF₆ and an excess amount of the desired ligand in dichloromethane solution. Both routes provided the target complexes in good yield and purity, allowing for their characterization by NMR (¹H and ³¹P) and IR spectroscopy.

Additionally, crystals of complexes 4–6 suitable for X-ray diffraction were obtained and their solid-state structures are presented in Figure 5, along with the structure of complex 2.¹⁹ With a series of complexes featuring varying auxiliary ligands in hand, we examined the performance of the ruthenium complexes as catalysts for the transfer hydrogenation of acetophenone. The conditions previously employed for complex 1 were used, and catalysis was allowed to proceed for 2 h. The amount of product formed at 1 and 2 h was quantified using ¹H NMR spectroscopy, and the turnover numbers (TON) at each time point are presented in Table 1. The data in Table 1 show that complexes 1, 2, and 5 display the highest activity for acetophenone transfer hydrogenation under basic conditions; the activities for complexes 4 and 6 were marginally lower. Interestingly, complex 3 is almost completely inactive under these conditions for transfer hydrogenation.

Similar to catalysis promoted by 1, where precipitation of 1-d emerges in the later stages of the reaction, catalytic experiments with 2 and 5 became purple and cloudy, consistent with formation of dimer 1-d. In contrast to the instability noted above, experiments performed with complexes 4 and 6 maintained homogeneity during catalysis and remained as bright orange-red solutions throughout the duration of the

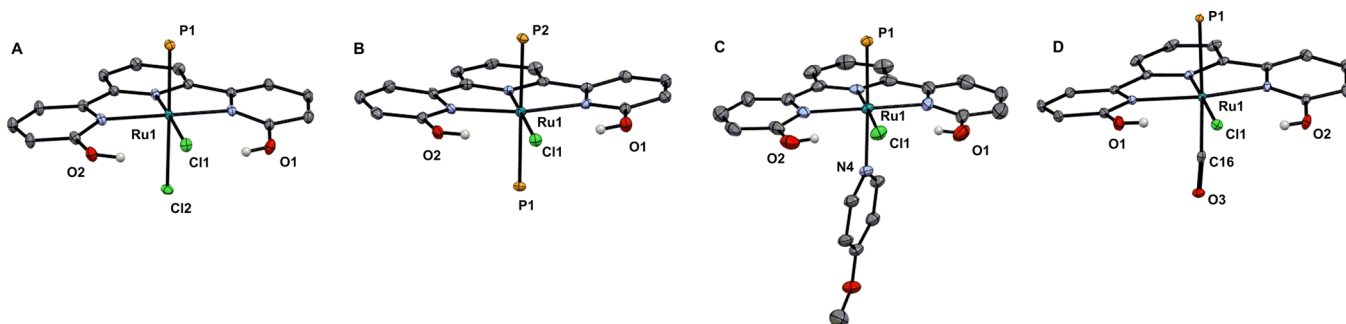


Figure 5. Solid-state structures of **2** (A), **3** (B), **5** (C), and **6** (D). (30% probability ellipsoids; PR₃ C atoms, H atoms not involved in hydrogen bonding, solvent, and counteranions omitted for clarity).

Table 1. Acetophenone Transfer Hydrogenation Catalyzed by Complexes **1–6**^a

catalyst	TON	
	1 h	2 h
1	141	159
2	108	124
3	9	16
4	91	106
5	120	138
6	62	107

^aConditions: Ru:KOtBu:ketone = 1:20:200, [iPrOH]₀ = 12.8 M, [acetophenone]₀ = 0.1 M, 80 °C.

experiment. Taken together, the data suggest that ruthenium-dhtp adducts featuring π -acidic auxiliary ligand sets display higher stability during catalysis. On the other hand, σ -donating ligand sets offer a catalytic system which has a higher activity for acetophenone reduction and suggests that an electron-rich ruthenium hydride species is required to facilitate insertion into the ketone substrate.

Although the σ -donating frameworks provide faster initial catalysis, they are plagued by the formation of **1-d**, due to the lability of the supporting ligands on ruthenium under basic conditions. This is likely a consequence of weak metal–ligand bonds between the electron-rich metal center (formed upon deprotonation of the dhtp ligand) and the σ -donating ligands.²⁰ One of the hallmarks of a desirable catalyst is stability, and therefore we narrowed our attention to complexes featuring π -acidic supporting ligands, which displayed high stability during catalysis. From the two complexes which fit this criterion (**4** and **6**), we chose to pursue mechanistic experiments with complex **6**, since the CO ligand provides a valuable signature for IR spectroscopy which could be used to gain insight into changes of electron density at the metal center (vide supra).

To further distinguish the reactivity profiles of complexes **1** and **6**, we examined the reduction of benzophenone catalyzed by these two complexes. We previously reported that complex **1** is unable to reduce this substrate (no conversion was observed after 12 h using our standard conditions), and we hypothesized this was due to steric constraints between the PPh₃ ligands and the incoming sterically imposing substrate.^{11a} Complex **6**, on the other hand, is able to reduce benzophenone to diphenylmethanol, providing 67% NMR yield after 16 h under identical conditions. These findings are consistent with a

catalytically active species which retains the auxiliary ligands coordinated to ruthenium.

Outer-Sphere Hydride Transfer Is the Rate-Limiting Step during Catalysis. On the basis of prior precedent, we envisioned two common, limiting mechanistic scenarios for ketone transfer hydrogenation catalyzed by complex **6**: (1) an inner-sphere hydride insertion pathway to coordinated substrate and (2) an outer-sphere delivery of hydride without substrate coordination.²¹ To distinguish between these two distinct mechanistic possibilities for catalysis, we performed kinetic analyses by monitoring reaction progress via ¹H NMR spectroscopy; either in situ or by collecting aliquots from reaction solutions at regular time intervals (see the Supporting Information for more details). Product (either acetone or 1-phenylethanol) concentrations were determined by integration using trimethyl(phenyl)silane as an internal standard, and all experiments were performed in triplicate to establish error.

A linear free energy analysis for transfer hydrogenation was conducted to first substantiate a rate-determining hydride transfer step and also to investigate the electronic character of the transition state during catalysis. A Hammett plot (Figure 6) was constructed by measuring the initial rates of reduction of para-substituted acetophenone substrates, which yielded a ρ value of +1.38(17). The dependence of the rate of ketone reduction on the σ value implicates a rate-determining hydride transfer to the ketone substrate. Moreover, the positive ρ value indicates buildup of negative charge on the ketone substrate

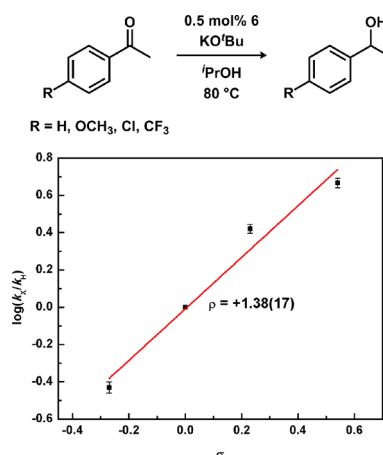


Figure 6. Hammett plot for transfer hydrogenation of substituted acetophenones catalyzed by **6**. Conditions: Ru:KOtBu:ketone = 1:20:200, [Ru] = 0.5 mM, [iPrOH]₀ = 12.4 M, [ketone]₀ = 0.1 M, [acetone]₀ = 0.5 M, 80 °C.

during the rate-determining step. The magnitude of ρ is consistent with hydride delivery to the ketone substrate in the transition state. This value is lower than that for the reduction of substituted acetophenones by NaBH_4 at 30 °C ($\rho = +2.02, +3.06$),²² reflecting a more anionic nature of the transition state for hydride transfer in the case of BH_4^- reduction.

To further evaluate a rate-limiting hydride transfer step, we performed kinetic analyses during catalysis. For a rate-determining hydride insertion pathway into coordinated substrate, a zero-order dependence of substrate concentration on the catalytic rate would be expected, since this step would involve a unimolecular insertion of hydride into substrate. Alternatively, for an outer-sphere hydride transfer, a first-order dependence on substrate would be predicted, since the transfer would involve a bimolecular reaction between the hydride source (ruthenium complex) and substrate. As such, we examined the effect of varying substrate concentration on the initial rate of acetophenone reduction to experimentally distinguish between these two limiting mechanistic regimes. As shown in Figure 7A, a first-order dependence on

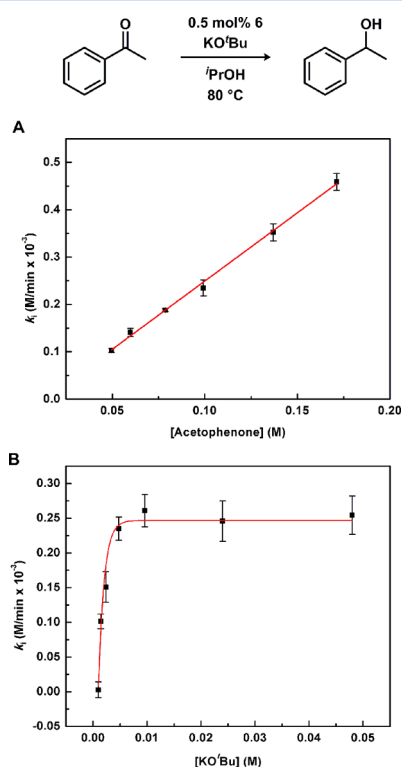


Figure 7. Dependence of acetophenone (A) and KO^tBu (B) concentrations on the initial rate of acetophenone transfer hydrogenation catalyzed by 6. Conditions: [Ru] = 0.5 mM, [acetone]₀ = 0.5 M, 80 °C.

acetophenone concentration is observed, which is consistent with a hydride transfer step from a ruthenium hydride species to a ketone substrate not located in the primary coordination sphere of the metal complex.

Base activation is a common step to initiate catalysis for transfer hydrogenation in order to generate catalytically active hydride species.²³ This commonly involves deprotonation of acidic groups on the ligand, such as the NH₂ groups for Noyori's catalyst. Catalytic cycles that are dependent on base activation typically exhibit saturation behavior; whereupon reaching a threshold of base concentration, the maximum

catalytic rate is achieved.^{4b,24} To determine whether base activation via deprotonation of the pendent OH groups precedes catalysis, we investigated the base dependence of acetophenone reduction using complex 6. As can be seen in Figure 7B, saturation behavior is observed and the maximum rate of acetophenone reduction is achieved at a ruthenium:base ratio of approximately 1:10.²⁵ Notably, no catalysis was observed in the absence of base. The saturation behavior could alternatively be explained by inhibition from ^tBuOH (generated from KO^tBu); however, added ^tBuOH has no effect on the reaction profile (Figure S4 in the Supporting Information). The base dependence is therefore most consistent with catalyst activation via deprotonation of the two OH groups on the dhtp scaffold, which turns on catalysis.

In order to analyze the activation parameters for catalysis and clarify the nature of the rate-determining transition state, an Eyring analysis was performed. For this study, 4-(trifluoromethyl)acetophenone was used as the ketone substrate, since appreciable rates for acetophenone reduction could not be observed at temperatures below 80 °C using our standard conditions.²⁶ The reaction rates were measured over a 40 °C window and fit to the Eyring equation (Figure 8) using

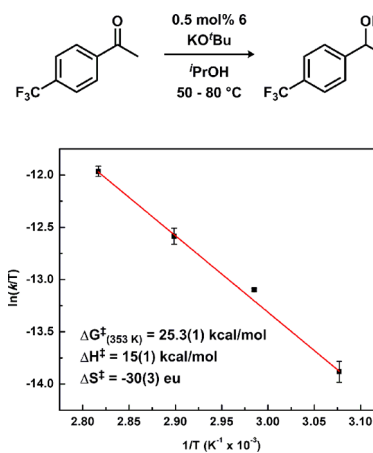


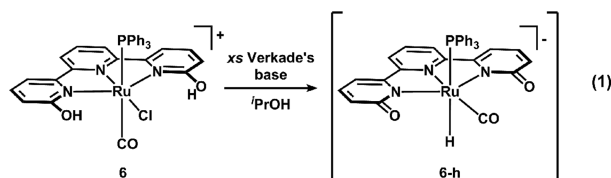
Figure 8. Eyring plot for the transfer hydrogenation of 4-(trifluoromethyl)acetophenone catalyzed by 6. Conditions: Ru:KO^tBu:4-trifluoromethylacetophenone = 1:20:200, [Ru] = 0.5 mM, [^tPrOH] = 12.8 M, [4-trifluoromethylacetophenone]₀ = 0.1 M, temperatures 50, 60, 70, and 80 °C.

the maximum linear, initial rate. This treatment provided $\Delta H^\ddagger = 15(1)$ kcal/mol and $\Delta S^\ddagger = -30(3)$ eu.²⁷ At 80 °C, these activation parameters correspond to a free energy of activation (ΔG^\ddagger) of 25.3(1) kcal/mol. The negative value of the activation entropy implies that an associative, higher-order process is operative during the rate-determining step.²⁰ In addition, the magnitude of the activation entropy is suggestive of a highly organized transition state involving association of substrate with the catalytically active species. In combination with the first-order substrate dependence and the Hammett studies, the kinetic data are consistent with rate-determining hydride transfer to the ketone substrate through a transition state which has a highly organized structure.

Alkali-Metal Cations Dictate the Rate of Acetophenone Reduction. The base employed in our studies (KO^tBu) contains an alkali-metal cation, which may or may not contribute to catalysis. Based on precedent from Noyori's system, which indicated a crucial role of alkali metals to achieve

efficient catalysis,⁸ we evaluated the potential role of the alkali-metal cation with complex **6**. In order to decouple the role of the base from that of the alkali-metal cation, we required a strong, neutral base which would generate ⁱPrO[−] anion in solution without any added metal cations. These conditions would allow us to directly probe whether or not alkali metals influence catalysis. To meet these criteria, we employed Verkade's base (2,8,9-triisopropyl-2,5,8,9-tetraaza-1-phosphabicyclo[3.3.3]undecane) to generate ⁱPrO[−] anion in solution and salts of the noncoordinating anions B(C₆F₅)₄[−] and B(C₈H₃F₆)₄[−] to introduce alkali-metal cations. Verkade's base is ideal for these purposes, since dissolution in ⁱPrOH quantitatively generates the corresponding phosphonium salt (R₃PH⁺, as determined by ³¹P NMR; Figure S5 in the Supporting Information), and presumably the ⁱPrO[−] counteranion. Moreover, the noncoordinating tetraarylborate anions should also be stable under the reaction conditions during catalysis.

Prior to performing catalysis, we investigated the reactivity of complex **6** with Verkade's base in ⁱPrOH. When a sample of **6** is suspended in ⁱPrOH (nondeuterated) and treated with excess (20 equiv) Verkade's base, the reaction mixture rapidly becomes homogeneous and orange. Analysis by ¹H and ³¹P NMR spectroscopy revealed that a new ruthenium hydride complex (**6-h**) formed (eq 1). The ¹H NMR spectrum of the



resulting solution shows that the resonances for the OH groups of the dhtp ligand have disappeared (which should be otherwise visible in nondeuterated, alcohol solvent in the absence of base) and a new doublet ($J_{HP} = 106$ Hz) hydride resonance at -8.91 ppm is present (Figure 9A, bottom spectrum). In addition, the ³¹P NMR spectrum of this reaction mixture exhibits two resonances (in addition to the PF₆[−] resonance): a doublet ($J_{PH} = 496$ Hz) at -11.73 ppm, corresponding to protonated Verkade's base, and a doublet ($J_{PH} = 105$ Hz) at 33.52 ppm, corresponding to the new ruthenium hydride species (Figure S7 in the Supporting Information). Note that free PPh₃ was not observed during the reaction of **6** with Verkade's base, consistent with retention of the PPh₃ ligand on ruthenium. On the basis of the magnitude of the coupling constant between the hydride and PPh₃ ligands, and the absence of dhtp OH resonances, the product is formulated as an anionic ruthenium hydride complex, in which the hydride ligand is trans-disposed to the PPh₃ ligand.²⁸ The formation of ruthenium hydride **6-h** likely proceeds through a transient five-coordinate intermediate (generated upon dehydrohalogenation of **6**) that readily abstracts hydride from ⁱPrO[−] anion in solution.

The position of the hydride resonance of **6-h** in the ¹H NMR spectrum is significantly affected by added alkali metals. For instance, addition of 20 equiv of Cs⁺ to a solution of **6-h** causes a downfield shift of ca. 0.3 ppm, whereas the addition of 20 equiv of Li⁺ to **6-h** induces an upfield shift of ca. 0.2 ppm (Figure 9A). The distinct shifting of the hydride resonance observed for each alkali metal provides support for alkali-metal association with the ruthenium complex in solution and

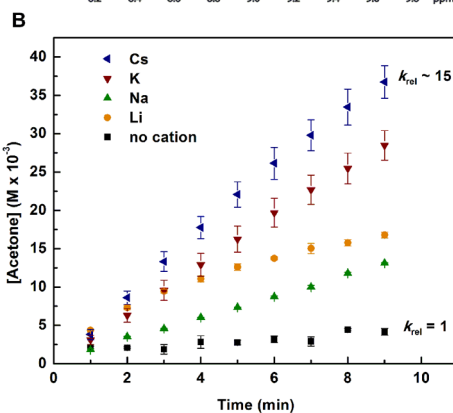
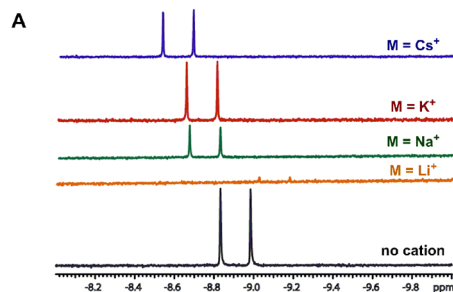
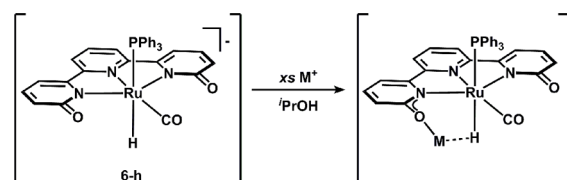


Figure 9. Binding of cations to **6-h**: hydride region of the 700 MHz ¹H NMR spectra of **6-h** in the presence of added cations (A) and initial reaction profiles for acetophenone transfer hydrogenation catalyzed by **6** in the presence of Verkade's base and alkali metals (B; conditions Ru:Verkade's base:cation:acetophenone = 1:20:20:200, [Ru] = 0.5 mM, [ⁱPrOH] = 12.8 M, [acetophenone]₀ = 0.1 M, 80 °C). Note that we do not imply a specific number of bound cations and the representation in this figure serves to illustrate how a single cation may associate with **6-h**.

suggests that the electronic character of the hydride is perturbed by the presence of alkali-metal cations. This finding is noteworthy, given the fact that these experiments are conducted in alcohol media, where alkali-metal cations are expected to be highly solvated.²⁹

In addition to altering the room-temperature NMR signature of the ruthenium hydride complex, alkali-metal cations dramatically impact the rate of acetophenone transfer hydrogenation. When acetophenone is heated to 80 °C in an ⁱPrOH solution containing 0.5 mol % of **6**, 10 mol % of Verkade's base, and 10 mol % of tetraarylborate salt, the rate of acetophenone reduction is dependent on the identity of the alkali-metal cation of the added salt. Salts of Li⁺, Na⁺, K⁺, and Cs⁺ were analyzed, and the initial reaction profiles are presented in Figure 9B. Comparison of the maximum initial rates for acetophenone reduction using Verkade's base/K⁺ cations ($k_i = [6.3(6)] \times 10^{-3}$ M/min) and KO^tBu ($k_i = [7.0(3)] \times 10^{-4}$ M/min) under identical conditions reveals that the combination of Verkade's base and K⁺ cations results in a significantly higher maximum initial rate, which may be due to differences in solution aggregation of KO^tBu or an increase in ionic strength.³⁰ The results presented in Figure 9B clearly demonstrate that the

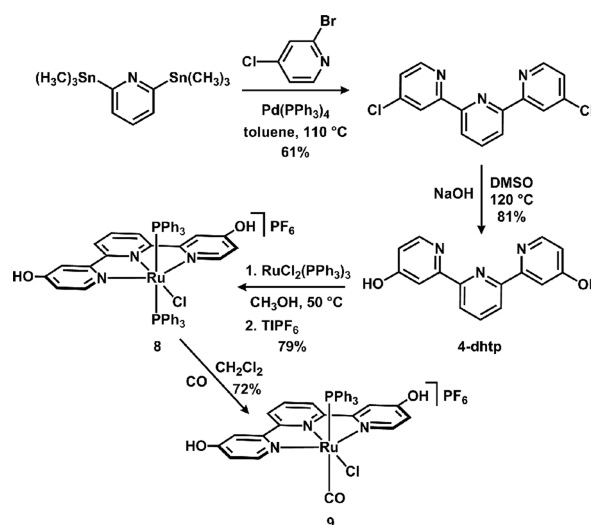
identity of the metal cation dictates the rate of reduction in the order $\text{Li} < \text{Na} < \text{K} < \text{Cs}$. This result has an important parallel to Noyori's catalyst, which also showed attenuated catalysis with increased cation Lewis acidity. In contrast, while the rate of catalysis of the Noyori system was greatest with K^+ (rationalized by substrate–cation– π interactions),⁸ this was not the case for **6**, whose rate further increased from K^+ to Cs^+ . Of additional importance, the maximum rate enhancement for complex **6** using Cs^+ (ca. 15-fold) exceeds that of Noyori's catalyst (ca. 4-fold),⁸ which strongly indicates that alkali-metal coordination plays a vital role in the present system.³¹ The rate enhancement is consistent with a change in electron density at the metal center upon binding the cation via an inductive effect, where the least electropositive cation provides the most electron rich metal center along the series. This notion is supported by the changes in chemical shift of the hydride resonance for **6-h** as a function of added alkali metal noted above.

Selectivity and Activity of the Catalyst Are Determined by the Location of the OH Groups. The dramatic cation dependence on catalytic activity implicates a transition state for hydride transfer that involves association of catalyst, cation, and substrate. The cation can bind to either the substrate or the catalyst, and the enhanced catalysis might be rationalized by distinct mechanistic scenarios to explain the experimental results: (1) the deprotonated alkoxide groups bind cations and organize substrate for hydride delivery within the secondary coordination sphere of the metal complex or (2) the excess cations in solution activate the ketone substrate for hydride attack in solution *removed from the metal center*. The former of these two limiting scenarios implies that the orientation of the OH groups on the ligand scaffold should affect the efficiency of catalysis, while if the latter were operative, the substitution pattern of the OH groups on the ligand scaffold should not significantly affect catalysis. In order to provide experimental evidence for either of these two scenarios, and clarify the proximity requirement of the alkoxide groups for catalysis, complexes analogous to **6** which (a) do not contain OH groups on the terpyridine ligand or (b) contain OH groups in a different position on the ligand were prepared. We examined two complexes identical with **6** which varied only with respect to the dhtp scaffold: the terpyridine complex ($\text{RuCl}(\text{CO})\text{terpy}(\text{PPh}_3)\text{PF}_6$ (**7**) and a new complex (**9**) featuring the 4,4'-dihydroxyterpyridine (4-dhtp) ligand (Scheme 2).

We employed IR spectroscopy to understand how the position of the OH groups on the terpyridine ligand would affect the electronics at the ruthenium center. Examination of the carbonyl stretching frequencies in the IR spectra of complexes **6** (2046 cm^{-1}) and **9** (2020 cm^{-1}) revealed that the protonated complexes present slightly different ligand fields to the ruthenium center, with complex **9** exhibiting a somewhat stronger ligand field. In contrast, the IR spectra in solution (CH_3OH) with excess base (Verkade's base, four equivalents) reveal that complexes **6** ($\nu_{\text{CO}} 1969\text{ cm}^{-1}$) and **9** ($\nu_{\text{CO}} 1970\text{ cm}^{-1}$) have nearly identical electronic environments at the ruthenium center (Figure S8 in the Supporting Information). These findings suggest that in basic, alcohol media, the ligand fields presented to the ruthenium center by dhtp and 4-dhtp are identical and that differences in catalytic activity under similar conditions are likely not attributable to electronic effects.

Although complexes **6** and **9** display comparable electronic environments in basic alcohol media, their activities for

Scheme 2. Synthesis of 4-dhtp and Ruthenium Complexes **8** and **9**



acetophenone transfer hydrogenation are dissimilar. When acetophenone is heated to $80\text{ }^\circ\text{C}$ in $i\text{PrOH}$ in the presence of 0.5 mol % of **6**, 10 mol % of Verkade's base and 10 mol % of $\text{KB}(\text{C}_6\text{F}_5)_4$, nearly complete conversion (191 turnovers) to 1-phenylethanol is achieved in 2 h. Under identical conditions, complex **9** provides 104 turnovers and complex **7**, featuring the parent terpyridine ligand, yields 34 turnovers (Table 2). These

Table 2. Acetophenone Transfer Hydrogenation Catalyzed by Complexes **6, **7**, and **9**^a**

catalyst	TON	
	1 h	2 h
6	163	191
7	17	34
9	83	104

^aConditions: Ru:Verkade's base:KB(C₆F₅)₄:acetophenone = 1:20:20:200, [*i*PrOH]₀ = 12.8 M, [acetophenone]₀ = 0.1 M, 80 °C.

results unambiguously establish that the presence of the OH groups on the terpyridine ligand increases catalytic activity and, moreover, that the position of the OH groups on the ligand dictates the overall efficiency.

Chemoselective reduction of ketone substrates which contain other sites of unsaturation is a hallmark of outer-sphere catalysis.^{21,32} To provide further support for a reduction mechanism in which alkali-metal binding activates and directs hydride insertion into the ketone, we examined the chemoselectivity of catalytic reductions. Previously, we reported that complex **1** was an inefficient catalyst for selectively reducing 5-hexen-2-one to 5-hexen-2-ol, providing only 44% selectivity³³ for the desired product. We hypothesized that this substrate would be ideal for benchmarking complexes **6**, **7**, and **9**, since product distributions can be used to assess general inner- or outer-sphere pathways for substrate reduction, where alkene reduction products likely arise from competitive inner-sphere pathways (note that we define an outer-sphere pathway as one that does not require substrate coordination directly to the

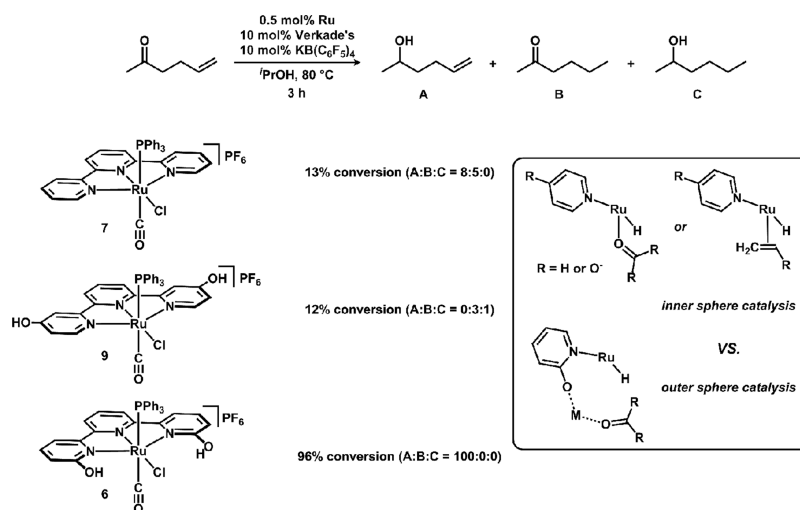


Figure 10. Chemoselectivity of transfer hydrogenation for complexes 6, 7, and 9 (conditions: Ru:Verkade's base:KB(C₆F₅)₄:ketone = 1:20:20:200, [ⁱPrOH]₀ = 12.8 M, [ketone]₀ = 0.1 M, 80 °C).

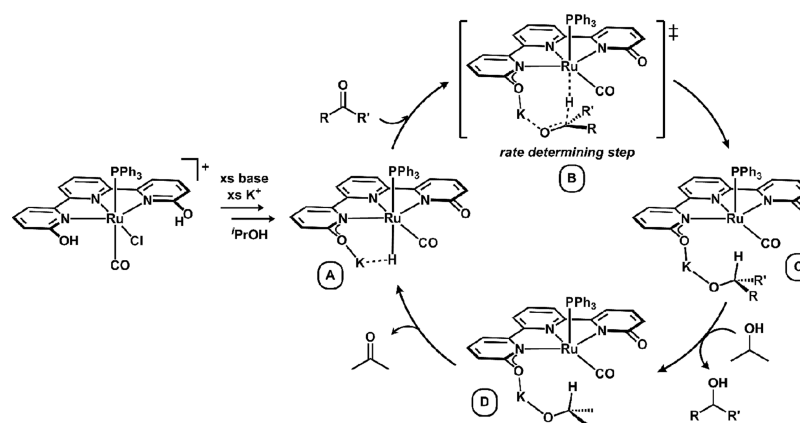


Figure 11. Proposed catalytic cycle for the transfer hydrogenation of ketones catalyzed by 6 under basic conditions in the presence of K⁺ ions.

metal center). When 5-hexen-2-one is subjected to the above transfer hydrogenation conditions using Verkade's base and KB(C₆F₅)₄ over 3 h, complexes 6, 7, and 9 display distinctive reactivity profiles. In the case of the parent terpyridine complex 7, 13% conversion of the starting ketone was noted and a mixture of carbonyl and olefin reduction products (A and B, respectively; Figure 10) was obtained in a 8:5 ratio, respectively.³⁴ However, in the case of the 4-dhtp complex 9, only the olefin reduction product and over-reduction product (C) were obtained in a 3:1 ratio with a total conversion from starting material of 12%. These findings are in stark contrast to reduction of this substrate by complex 6, which proceeded to 96% conversion, yielding exclusively the carbonyl reduction product (A).

While the position of the OH groups on the ligand scaffold dictated the *efficiency* of catalysis in the case of acetophenone, the OH groups similarly dictate the *selectivity* of catalysis when a substrate such as 5-hexen-2-one is used. This result further exemplifies the utility of the 2-hydroxypyridine motif for catalysis. The chemoselectivity data presented here are consistent with two distinct mechanistic regimes operative for complex 6 and complexes 7 and 9. The ability of complexes 7 and 9 to reduce olefin substrates suggests that hydride insertion into substrate is nonselective and that two competing mechanisms (insertion into coordinated substrate and hydride

transfer to outer-sphere substrate) are operative (Figure 10 inset). In combination with the alkali-metal dependence, the selectivity of complex 6, on the other hand, suggests that, when deprotonated, the pendent alkoxide groups are responsible for orienting substrate for hydride transfer in an outer-sphere pathway.

Ketone Reduction Involves Preorganization of Substrate through Alkali-Metal Coordination. A unified mechanism for ketone transfer hydrogenation catalyzed by complex 6 is proposed in Figure 11. Entrance into the catalytic cycle begins with the formation of the hydride complex (A), via a dehydrohalogenation reaction, upon introduction of base and cation (in this case K⁺) in ⁱPrOH solution. This step is supported by NMR characterization of complex 6-h, as well as through the demonstration of alkali-metal association to this species in ⁱPrOH solution. Following hydride formation, attack on the substrate proceeds through an intermediate (B) in which the carbonyl group is polarized through interaction with K⁺. Key data to support this supposition are the observed cation effects on reduction rate and large, negative entropy of activation (−30 eu), supporting a highly organized, associative transition state during hydride delivery.³⁵ Upon hydride attack on the carbonyl, we postulate that a K⁺-bound alkoxide (C) is formed, in analogy to Noyori's catalyst as described by several research groups.^{9,10} Protonolysis of the alkoxide C with ⁱPrOH

to release substrate provides D and the catalytic cycle is closed following hydride abstraction from isopropyl alcohol in complex D, liberating acetone. In this catalytic cycle, the cation plays a key role in increasing activity in two respects: (1) polarizing the carbonyl group of the ketone through coordination and (2) orienting the ketone substrate for hydride transfer.

CONCLUSIONS

In conclusion, we have demonstrated remarkable differences in selectivity and activity for transfer hydrogenation that are imparted by pendent OH groups. Deprotonation of the OH groups modulates the electronics at the metal center, providing a more electron rich ruthenium center under basic conditions. The location of the resulting alkoxide groups serves to orient the ketone substrate through ion pairing with alkali metals. This ion pairing facilitates chemoselective transfer hydrogenation of ketones in the presence of olefins. We note that the presently observed role of cations may well be operative in other 2-hydroxypyridine catalysts that function under highly basic conditions in the presence of high concentrations of alkali metals.^{11j,m,36} The results here illustrate that a simple ligand modification (installation of OH groups in the 2-position of a pyridine ring) imparts dramatic changes to catalysis. They turn on catalysis through electronic perturbations at the metal site and, importantly, can change the mechanism of catalysis (switching from inner-sphere to outer-sphere pathways). Thus, we term the modification as a general alkoxide effect and note that the design principles described herein should be valuable tools when constructing future ligand ensembles for catalysis.

ASSOCIATED CONTENT

Supporting Information

The Supporting Information is available free of charge on the ACS Publications website at DOI: 10.1021/acscatal.6b00229.

Synthetic and experimental procedures, NMR spectra, and representative kinetic data (PDF)

Crystallographic data (CIF)

AUTHOR INFORMATION

Corresponding Author

*E-mail for N.K.S.: nszym@umich.edu.

Notes

The authors declare no competing financial interest.

ACKNOWLEDGMENTS

This work was supported by the University of Michigan Department of Chemistry, an NSF-CAREER grant (CHE-1350877), an NSF-GRFP grant (C.M.M.), the UM Rackham Graduate School (C.M.M.), and the NSF (CHE-0840456) for X-ray instrumentation. N.K.S. is a Dow Corning Assistant Professor and Alfred P. Sloan Research Fellow. We thank Dr Jeff W. Kampf for X-ray assistance and Boulder Scientific Co. for a generous donation of LiB(C₆F₅)₄.

REFERENCES

- (1) (a) Crabtree, R. H. *New J. Chem.* **2011**, *35*, 18–23. (b) Gunanathan, C.; Milstein, D. *Acc. Chem. Res.* **2011**, *44*, 588–602.

- (2) (a) Ohkuma, T.; Ooka, H.; Hashiguchi, S.; Ikariya, T.; Noyori, R. *J. Am. Chem. Soc.* **1995**, *117*, 2675–2676. (b) Ohkuma, T.; Ooka, H.; Ikariya, T.; Noyori, R. *J. Am. Chem. Soc.* **1995**, *117*, 10417–10418. (c) Noyori, R.; Sandoval, C. A.; Muniz, K.; Ohkuma, T. *Philos. Trans. R. Soc., A* **2005**, *363*, 901–912. (d) Noyori, R.; Yamakawa, M.; Hashiguchi, S. *J. Org. Chem.* **2001**, *66*, 7931–7944. (e) Noyori, R. *Angew. Chem., Int. Ed.* **2002**, *41*, 2008–2022.

- (3) For selected recent examples, see: (a) Schmeier, T. J.; Dobereiner, G. E.; Crabtree, R. H.; Hazari, N. *J. Am. Chem. Soc.* **2011**, *133*, 9274–9277. (b) Bartoszewicz, A.; Marcos, R.; Sahoo, S.; Inge, A. K.; Zou, X.; Martin-Matute, B. *Chem. - Eur. J.* **2012**, *18*, 14510–14519. (c) Kashiwame, Y.; Kuwata, S.; Ikariya, T. *Organometallics* **2012**, *31*, 8444–8455. (d) Yoshinari, A.; Tazawa, A.; Kuwata, S.; Ikariya, T. *Chem. - Asian J.* **2012**, *7*, 1417–1425. (e) Bichler, B.; Holzhaecker, C.; Stoeger, B.; Puchberger, M.; Veiros, L. F.; Kirchner, K. *Organometallics* **2013**, *32*, 4114–4121. (f) Hulley, E. B.; Helm, M. L.; Bullock, R. M. *Chem. Sci.* **2014**, *5*, 4729–4741. (g) Kuwata, S.; Ikariya, T. *Chem. Commun.* **2014**, *50*, 14290–14300. (h) Toda, T.; Kuwata, S.; Ikariya, T. *Chem. - Eur. J.* **2014**, *20*, 9539–9542. (i) Marelus, D. C.; Darrow, E. H.; Moore, C. E.; Golen, J. A.; Rheingold, A. L.; Grotjahn, D. B. *Chem. - Eur. J.* **2015**, *21*, 10988–10992. (j) Grotjahn, D. B.; Kragulj, E. J.; Zeinalipour-Yazdi, C. D.; Miranda-Soto, V.; Lev, D. A.; Cooksy, A. L. *J. Am. Chem. Soc.* **2008**, *130*, 10860–10861. (k) Kawahara, R.; Fujita, K.-i.; Yamaguchi, R. *Angew. Chem., Int. Ed.* **2012**, *51*, 12790–12794.

- (4) (a) Hayes, J. M.; Deydier, E.; Ujaque, G.; Lledos, A.; Malacea-Kabbara, R.; Manoury, E.; Vincendeau, S.; Poli, R. *ACS Catal.* **2015**, *5*, 4368–4376. (b) Mikhailine, A. A.; Maishan, M. I.; Lough, A. J.; Morris, R. H. *J. Am. Chem. Soc.* **2012**, *134*, 12266–12280. (c) Zhang, G.; Vasudevan, K. V.; Scott, B. L.; Hanson, S. K. *J. Am. Chem. Soc.* **2013**, *135*, 8668–8681. (d) Lagaditis, P. O.; Sues, P. E.; Lough, A. J.; Morris, R. H. *Dalton Trans.* **2015**, *44*, 12119–12127. (e) Sonnenberg, J. F.; Coombs, N.; Dube, P. A.; Morris, R. H. *J. Am. Chem. Soc.* **2012**, *134*, 5893–5899.

- (5) (a) Suna, Y.; Ertem, M. Z.; Wang, W.-H.; Kambayashi, H.; Manaka, Y.; Muckerman, J. T.; Fujita, E.; Himeda, Y. *Organometallics* **2014**, *33*, 6519–6530. (b) Wang, W.-H.; Hull, J. F.; Muckerman, J. T.; Fujita, E.; Himeda, Y. *Energy Environ. Sci.* **2012**, *5*, 7923–7926. (c) Zeng, G.; Sakaki, S.; Fujita, K.-i.; Sano, H.; Yamaguchi, R. *ACS Catal.* **2014**, *4*, 1010–1020. (d) Wang, W.-H.; Muckerman, J. T.; Fujita, E.; Himeda, Y. *ACS Catal.* **2013**, *3*, 856–860.

- (6) (a) Noyori, R.; Kitamura, M.; Ohkuma, T. *Proc. Natl. Acad. Sci. U. S. A.* **2004**, *101*, 5356–5362. (b) Phillips, S. D.; Fuentes, J. A.; Clarke, M. L. *Chem. - Eur. J.* **2010**, *16*, 8002–8005. (c) Zhao, B.; Han, Z.; Ding, K. *Angew. Chem., Int. Ed.* **2013**, *52*, 4744–4788.

- (7) Sandoval, C. A.; Ohkuma, T.; Muniz, K.; Noyori, R. *J. Am. Chem. Soc.* **2003**, *125*, 13490–13503.

- (8) Hartmann, R.; Chen, P. *Angew. Chem., Int. Ed.* **2001**, *40*, 3581–3585.

- (9) (a) Hamilton, R. J.; Leong, C. G.; Bigam, G.; Miskolzie, M.; Bergens, S. H. *J. Am. Chem. Soc.* **2005**, *127*, 4152–4153. (b) Hamilton, R. J.; Bergens, S. H. *J. Am. Chem. Soc.* **2006**, *128*, 13700–13701. (c) Hamilton, R. J.; Bergens, S. H. *J. Am. Chem. Soc.* **2008**, *130*, 11979–11987. (d) Takebayashi, S.; Dabral, N.; Miskolzie, M.; Bergens, S. H. *J. Am. Chem. Soc.* **2011**, *133*, 9666–9669. (e) John, J. M.; Takebayashi, S.; Dabral, N.; Miskolzie, M.; Bergens, S. H. *J. Am. Chem. Soc.* **2013**, *135*, 8578–8584.

- (10) Dub, P. A.; Henson, N. J.; Martin, R. L.; Gordon, J. C. *J. Am. Chem. Soc.* **2014**, *136*, 3505–3521.

- (11) (a) Moore, C. M.; Szymczak, N. K. *Chem. Commun.* **2013**, *49*, 400–402. (b) Tutusaus, O.; Ni, C.; Szymczak, N. K. *J. Am. Chem. Soc.* **2013**, *135*, 3403–3406. (c) Moore, C. M.; Szymczak, N. K. *Chem. Commun.* **2015**, *51*, 5490–5492. (d) Wang, W.-H.; Muckerman, J. T.; Fujita, E.; Himeda, Y. *New J. Chem.* **2013**, *37*, 1860–1866. (e) Fujita, K.-i.; Ito, W.; Yamaguchi, R. *ChemCatChem* **2014**, *6*, 109–112. (f) Fujita, K.-i.; Tanaka, Y.; Kobayashi, M.; Yamaguchi, R. *J. Am. Chem. Soc.* **2014**, *136*, 4829–4832. (g) Wang, W.-H.; Himeda, Y.; Muckerman, J. T.; Fujita, E. *Adv. Inorg. Chem.* **2014**, *66*, 189–222. (h) Nieto, I.; Livings, M. S.; Sacci, J. B.; Reuther, L. E.; Zeller, M.;

- Papish, E. T. *Organometallics* **2011**, *30*, 6339–6342. (i) DePasquale, J.; Nieto, I.; Reuther, L. E.; Herbst-Gervasoni, C. J.; Paul, J. J.; Mochalin, V.; Zeller, M.; Thomas, C. M.; Addison, A. W.; Papish, E. T. *Inorg. Chem.* **2013**, *52*, 9175–9183. (j) Gerlach, D. L.; Bhagan, S.; Cruce, A. A.; Burks, D. B.; Nieto, I.; Truong, H. T.; Kelley, S. P.; Herbst-Gervasoni, C. J.; Jernigan, K. L.; Bowman, M. K.; Pan, S.; Zeller, M.; Papish, E. T. *Inorg. Chem.* **2014**, *53*, 12689–12698. (k) Marelus, D. C.; Bhagan, S.; Charboneau, D. J.; Schroeder, K. M.; Kamdar, J. M.; McGettigan, A. R.; Freeman, B. J.; Moore, C. E.; Rheingold, A. L.; Cooksy, A. L.; Smith, D. K.; Paul, J. J.; Papish, E. T.; Grotjahn, D. B. *Eur. J. Inorg. Chem.* **2014**, *2014*, 676–689. (l) Fujita, K.-i.; Kawahara, R.; Aikawa, T.; Yamaguchi, R. *Angew. Chem., Int. Ed.* **2015**, *54*, 9057–9060. (m) Zhang, T.; Wang, C.; Liu, S.; Wang, J.-L.; Lin, W. *J. Am. Chem. Soc.* **2014**, *136*, 273–281. (n) Dimondo, D.; Thibault, M. E.; Britten, J.; Schlaf, M. *Organometallics* **2013**, *32*, 6541. (o) Geri, J. B.; Szymczak, N. K. *J. Am. Chem. Soc.* **2015**, *137*, 12808–12814. (p) Chakraborty, S.; Piszal, P. E.; Brennessel, W. W.; Jones, W. D. *Organometallics* **2015**, *34*, 5203–5206.
- (12) Moore, C. M.; Dahl, E. W.; Szymczak, N. K. *Curr. Opin. Chem. Biol.* **2015**, *25*, 9–17.
- (13) Lancaster, K. M. *Struct. Bonding (Berlin, Ger.)* **2011**, *142*, 119–153.
- (14) Manbeck, G. F.; Muckerman, J. T.; Szalda, D. J.; Himeda, Y.; Fujita, E. *J. Phys. Chem. B* **2015**, *119*, 7457–7466.
- (15) Sullivan, B. P.; Calvert, J. M.; Meyer, T. J. *Inorg. Chem.* **1980**, *19*, 1404–1407.
- (16) Letko, C. S.; Rauchfuss, T. B.; Zhou, X.; Gray, D. L. *Inorg. Chem.* **2012**, *51*, 4511–4520.
- (17) Chu, W.-Y.; Zhou, X.; Rauchfuss, T. B. *Organometallics* **2015**, *34*, 1619–1626.
- (18) Note that heating **1-d** with excess PPh₃ at 80 °C did not result in any reaction, highlighting the stability of this complex.
- (19) Please see the [Supporting Information](#) for more details.
- (20) Hartwig, J. F. *Organotransition Metal Chemistry*; University Science Books: Mill Valley, CA, 2010.
- (21) Clapham, S. E.; Hadzovic, A.; Morris, R. H. *Coord. Chem. Rev.* **2004**, *248*, 2201–2237.
- (22) (a) Bowden, K.; Hardy, M. *Tetrahedron* **1966**, *22*, 1169–1174. (b) Mullins, R. J.; Vedernikov, A.; Viswanathan, R. *J. Chem. Educ.* **2004**, *81*, 1357.
- (23) Abdur-Rashid, K.; Clapham, S. E.; Hadzovic, A.; Harvey, J. N.; Lough, A. J.; Morris, R. H. *J. Am. Chem. Soc.* **2002**, *124*, 15104–15118.
- (24) Baratta, W.; Siega, K.; Rigo, P. *Chem. - Eur. J.* **2007**, *13*, 7479–7486.
- (25) Note that, at high base concentrations, the background KO^tBu-catalyzed Meerwein–Ponndorf–Verley reduction of acetophenone was subtracted.
- (26) Note that a linear Hammett plot indicates that the rate-limiting step during catalysis is unchanged upon modifying the substrate.
- (27) Morse, P. M.; Spencer, M. D.; Wilson, S. R.; Girolami, G. S. *Organometallics* **1994**, *13*, 1646–1655.
- (28) Reade, S. P.; Nama, D.; Mahon, M. F.; Pregosin, P. S.; Whittlesey, M. K. *Organometallics* **2007**, *26*, 3484–3491.
- (29) Note that differences in coordination environment across the alkali metals are likely, and the precise aggregation/solvation state may be complex.
- (30) Protonated Verkade's base (R₃PH⁺) is unlikely to perturb the reaction profile, given the stability of the P–H bond and the steric constraints imposed by the ^tPr groups. A search of the Cambridge Structural Database for similar R₃PH⁺ cations revealed that the P–H units in these structures do not engage in intramolecular interactions (i.e. hydrogen bonds) with hydrogen bond acceptors such as Cl[−] and phosphonates. For an example, please see: Chintareddy, V. R.; Ellern, A.; Verkade, J. G. *J. Org. Chem.* **2010**, *75*, 7166–7174.
- (31) The catalytic profile for Li⁺ is distinct among the other alkali metals, similar to the ¹H NMR signatures of the hydride noted above, and this may be a further consequence of differences in solution aggregation/solvation.
- (32) (a) Noyori, R.; Ohkuma, T. *Angew. Chem., Int. Ed.* **2001**, *40*, 40–73. (b) Casey, C. P.; Guan, H. *J. Am. Chem. Soc.* **2007**, *129*, 5816–5817. (c) Mikhailine, A.; Lough, A. J.; Morris, R. H. *J. Am. Chem. Soc.* **2009**, *131*, 1394–1395.
- (33) The selectivity could be increased by adding PPh₃ to the reaction mixture, which likely suppresses a competitive inner-sphere reduction pathway.^{11a}
- (34) Note that C=C bond migration from product A may provide product B. At this time we cannot unequivocally rule out this pathway. However, such a pathway implies an inner-sphere pathway of hydride delivery to substrate for complexes **7** and **9**.
- (35) For a related proposed transition state involving an alkali-metal cation during transfer hydrogenation, see: Wettergren, J.; Buitrago, E.; Ryberg, P.; Adolfsson, H. *Chem. - Eur. J.* **2009**, *15*, 5709–5718.
- (36) Hull, J. F.; Himeda, Y.; Wang, W.-H.; Hashiguchi, B.; Periana, R.; Szalda, D. J.; Muckerman, J. T.; Fujita, E. *Nat. Chem.* **2012**, *4*, 383–388.